The Astrophysical Journal, 850:165 (5pp), 2017 December 1 https://doi.org/10.3847/1538-4357/aa960d

The Detection of 6.9 μm Emission Features in the Infrared Spectra of IRAS 04296+3429, IRAS 05341+0852, and IRAS 22272+5435: Evidence for the Presence of H_n-PAHs in Post-AGB Stars

Christopher K. Materese[1,2], Jesse D. Bregman[1], and Scott A. Sandford[1]
[1] NASA-Ames Research Center, Mail Stop 245-6, Moffett Field, CA 94035, USA; Scott.A.Sandford@nasa.gov
[2] Bay Area Environmental Research Institute, 625 2nd Street, Suite 209, Petaluma, CA 94952, USA
Received 2017 March 9; revised 2017 September 15; accepted 2017 October 5; published 2017 November 28

Abstract

Polycyclic aromatic hydrocarbons (PAHs) are generally believed to be ubiquitous in space and responsible for numerous telltale interstellar infrared emission bands. In Sandford et al., we suggested that PAHs with excess hydrogenation at their periphery (H_n-PAHs) may be an important subclass of these molecules in some astrophysical environments. These molecules are candidates to explain objects with anomalously large 3.4 μm features, which are presumed to be associated with the aliphatic C–H stretching vibrations of the excess hydrogen. In that work, we suggest that for H_n-PAHs to be a viable candidate as the source for this 3.4 μm feature, we must also expect to observe methylene scissoring modes at 6.9 μm. In this work, we continue to develop the H_n-PAH hypothesis with a focus on the 6.9 μm feature. We also present some new observations of three post-asymptotic giant branch (post-AGB) objects with abnormally large 3.4 μm features, IRAS 04296+3429, IRAS 05341+0852, and IRAS 22272+5435, in addition to one post-AGB object with normal PAH emissions, IRAS 20000+3239. These observations were made using the FORCAST instrument in grism mode on the Stratospheric Observatory for Infrared Astronomy aircraft and demonstrate the presence of a 6.9 μm feature for the three objects with abnormally large 3.4 μm features and no detectable 6.9 μm feature for the normal PAH emitter. These results are consistent with the hypothesis that H_n-PAHs are a possible source of these infrared emission bands.

Key words: infrared: ISM – ISM: lines and bands – ISM: molecules – molecular data

Supporting material: data behind figures

1. Introduction

Polycyclic aromatic hydrocarbons (PAHs) are aromatic multiringed molecules with delocalized π-electron systems that make them extremely resilient against UV-photodestruction. These molecules, their ions, and related compounds are believed to be responsible for a number of interstellar emission features, the largest of which fall at 3.3, 6.2, 7.7, 8.7, 11.3, and 12.7 μm (Allamandola et al. 1989a, 1989b, 1999; Peeters et al. 2002; Tielens 2008). The general composition of a given population of PAHs is highly dependent on the environment in which it originated. The variations in the population of PAHs may include differing ring sizes, the integration of heteroatoms, differing ionization states, the addition of functionalized side groups, and deficits or excesses of peripherial hydrogen atoms.

We have previously proposed that PAHs with excess peripheral hydrogenation (H_n-PAHs) may be an important subclass of these molecules (Sandford et al. 2013). H_n-PAHs maintain a cyclic structure and contain some aromatic domains like their parent PAHs, but they also possess aliphatic methylene (–CH_2–) domains that disrupt the π-networks. Consequently, the aliphatic domains in H_n-PAHs are expected to be far more susceptible to UV-photodestruction, and therefore are shorter lived in many environments in space.

While PAHs largely consist of locally planar sheets of fused carbon rings, the aliphatic carbons in H_n-PAHs break this planarity. The presence of neighboring planar and tetrahedral moieties creates molecular strain that can have significant effects on the infrared spectrum. It should be noted that simple cyclic aliphatic compounds (i.e., compounds with no aromatic moieties) are already strained relative to their linear aliphatic counterparts. This type of strain tends to slightly blueshift aliphatic C–H stretch bands near 3.4 μm in H_n-PAHs relative to their canonical positions (Silverstein & Bassler 1967). Molecular symmetries are often broken in H_n-PAHs, leading to an increase in infrared (IR) active modes relative to the parent PAH. Notably, the intrinsic band strength of an aliphatic C–H stretch is typically two to three times stronger than that of an aromatic C–H stretch (Wexler 1967). Consequently, relatively few aliphatic domains in a given H_n-PAH can provide a very strong aliphatic C–H stretch feature near 3.4 μm relative to the aromatic C–H stretch feature near 3.3 μm.

We previously suggested that H_n-PAHs are an especially attractive candidate to partially explain the anomalously large 3.4 μm feature observed in some post-asymptotic giant branch (post-AGB) objects (Sandford et al. 2013). In that work, we compared our laboratory spectra of Ar matrix isolated H_n-PAHs to the emission spectra of a normal PAH emitter (IRAS 21282+5050) and two post-AGB objects (IRAS 22272+5435 and IRAS 04296+3429). In both IRAS 22272+5435 and IRAS 04296+3429, the strongest part of the 3.4 μm emission feature corresponded with a slightly blueshifted –CH_2– asymmetric stretch with much lower absorption at the canonical –CH_3 asymmetric stretch position. This suggests that strained methylene groups were the dominant type of aliphatic material in these objects, consistent with the H_n-PAH hypothesis. If H_n-PAHs, or more generally, methylene groups are a significant component of the 3.4 μm feature as suggested, it follows that other methylene related emission features should be observable in the infrared spectra of these objects and their detection would help corroborate this hypothesis. One such feature associated with a –CH_2– scissoring mode appears at

6.9 μm. In Sandford et al. (2013), we noted that this feature appears in emission spectra of both IRAS 22272+5435 and IRAS 04296+3429 (PAH emitters with anomalously large 3.4 μm features), but is absent in the spectrum of IRAS 21282 +5050 (a normal PAH emitter).

In general, post-AGB objects are relatively dim in the mid-IR (3–8 μm) making observations of these objects more difficult. Few high-quality spectra of these objects in the region encompassing the 6.9 μm feature are available for analysis. In this work, we discuss the implications of the H_n-PAH hypothesis as it relates to the 6.9 μm feature. Additionally, we present new observational data in the 5.34–7.61 μm range of three (post-AGB) objects with abnormally large 3.4 μm features, IRAS 04296+3429, IRAS 05341 +0852, and IRAS 22272+5435, as well as one post-AGB object with normal PAH emissions, IRAS 20000+3239. These observations were made using the Stratospheric Observatory for Infrared Astronomy (SOFIA; Adams et al. 2010).

2. Observation

Spectra were obtained from SOFIA (Young et al. 2012) using the FORCAST instrument (Herter et al. 2012) in the cross-dispersed grism mode (FOR_XG063), providing a spectral resolution of 1200 from 4.95 to 7.65 μm. We were supplied flux calibrated data for all the observed sources, and the details of the reduction procedure can be found in the FORCAST Guest Investigator's Handbook (https://www.sofia.usra.edu/sites/default/files/FORCAST_GI_Handbook_RevB.pdf).

The level three data consists of the spectra from eight orders of the grating spread across the detector, and delivered to observers as a 252 × 5 × 8 array. For each order (the third index of the array), the wavelength is in the first column, the flux (in Jansky) is in the second column, and the error is in the third column. Since grating efficiency is poor at the ends of the spectra, we deleted data points with a signal-to-noise less than three before combining the orders to form a single spectrum. This procedure also deleted data points shortward of 5.34 μm, where the stellar fluxes are low. The signal-to-noise ratio (S/N) of the observations was found to be less than expected, so we performed a 10-point binning of the data, which reduced the spectral resolution to 120 but improved the S/N. The observational results are presented along with previously published 3 μm reference data in the following figures: IRAS 20000+3239 (Figures 1(a), (b)), IRAS 04296+3429 (Figures 2(a), (b)), IRAS 05341+0852 (Figures 3(a), (b)), and IRAS 22272+5435 (Figures 4(a), (b)).

3. Discussion

PAHs have no significant infrared active bands at 6.9 μm; and consequently, normal PAH emission objects are not predicted to have significant emission features at that wavelength. IRAS 20000+3239 was selected for observation because it is categorized as a normal PAH emitter and serves the role of a control for this study. In contrast, (–CH_2–) domains in H_n-PAHs produce detectable bands at 6.9 μm (Sandford et al. 2013) that are accompanied by corresponding aliphatic stretching bands near 3.4 μm. IRAS 04296+3429, IRAS 05341+0852, and IRAS 22272+5435 were all selected for observations because they were known to have abnormally large 3.4 μm features relative to their 3.3 μm bands (Geballe et al. 1992; Goto et al. 2007 and Geballe et al. 1992, respectively). Although previous observational data that covered the 6.9 μm feature were available for both IRAS 04296+3429 (*Spitzer* IRS IrsStare as part of the Deuterium Enrichment in PAHs program Request key: 4116736, observation date: 2007-02-05T20:18:27) and IRAS 22272+5435 (*ISO* SWS 01 as part of the PROCHE.STARDUST proposal observation ID: 36601502, observation date: 1996-11-17T02:39:12), as was discussed in Sandford et al. (2013); to our knowledge, this was the first attempt to observe these objects along with a normal PAH emitter during a single observational window on the same instrument under the same conditions.

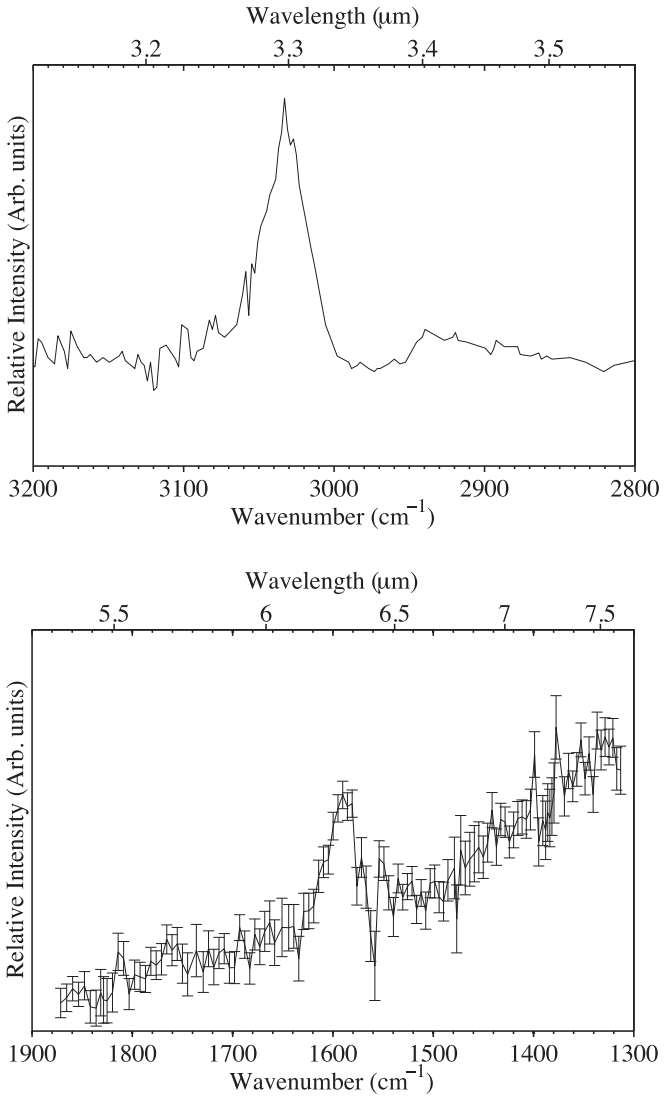

Figure 1. Infrared emission spectra of IRAS 20000+3239. (Top) 3.3 and 3.4 μm features from Hrivnak et al. (2007). (Bottom) 5.34–7.61 μm SOFIA spectral observations. The data used to create this figure are available.

As predicted, the spectrum of IRAS 20000+3239 (Figure 1(b)) shows the expected 6.2 μm PAH band that is consistent with a type B (defined as an object whose 6.2 μm band position falls between 6.235 and 6.28 μm) PAH emitter (Peeters et al. 2002), but shows no evidence of any detectable features at 6.9 μm. In contrast, although the signal-to-noise ratios for the spectra were both somewhat low, both a 6.2 μm

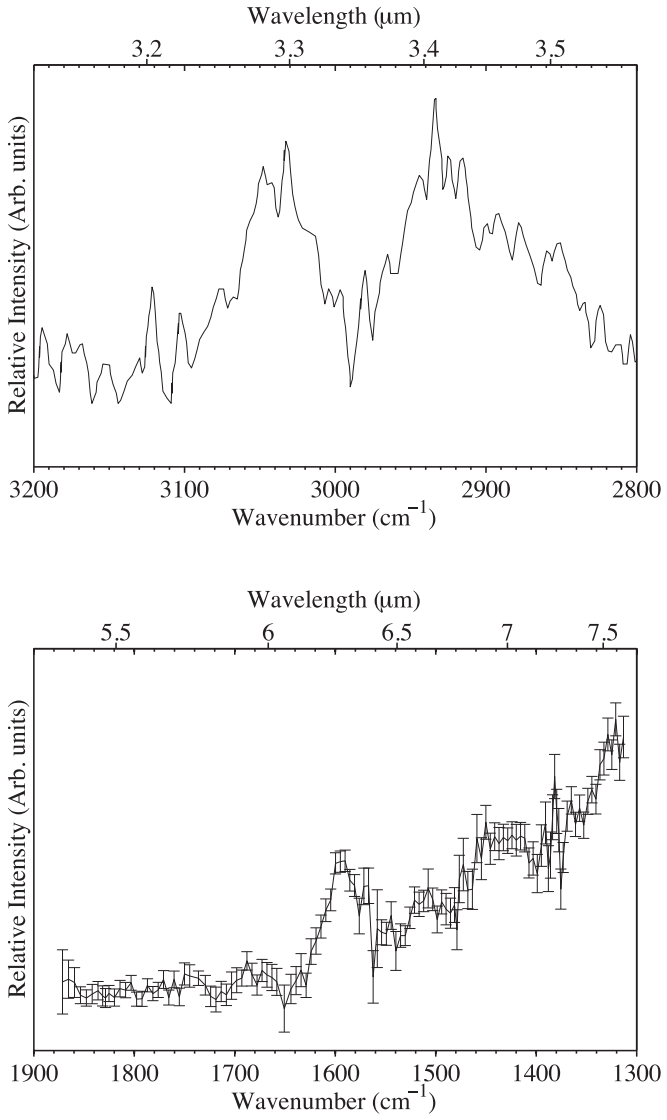

Figure 2. Infrared emission spectra of IRAS 04296+3429. (Top) 3.3 and 3.4 μm features from Geballe et al. (1992). (Bottom) 5.34–7.61 μm SOFIA spectral observations. The data used to create this figure are available.

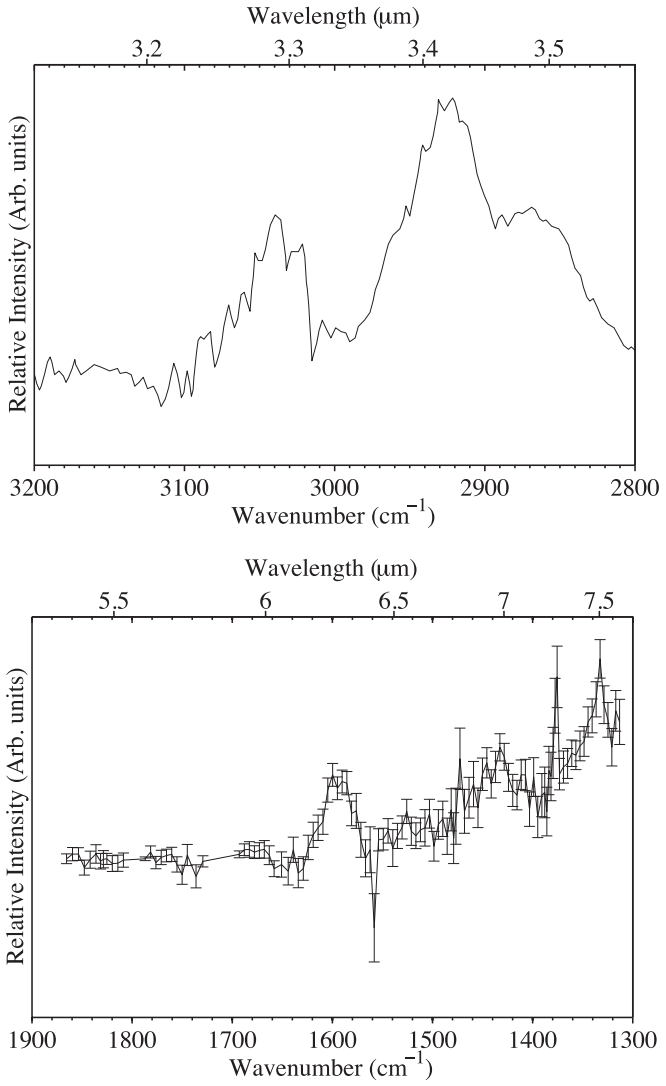

Figure 3. Infrared emission spectra of IRAS 05341+0852. (Top) 3.3 and 3.4 μm features from Goto et al. (2007). (Bottom) 5.34–7.61 μm SOFIA spectral observations. The data used to create this figure are available.

PAH feature as well as a 6.9 μm feature are readily apparent in the spectra of both IRAS 04296+3429 (Figure 2(b)) and IRAS 05341+0852 (Figure 3(b)). The signal-to-noise for IRAS 22272+5435 (Figure 4(b)) was far better than for any of the other objects observed and shows very clear features at both 6.2 and 6.9 μm. Although the presence of the 6.9 μm feature is consistent with the presence of methylene groups, that alone is not a definitive identification of H_n-PAHs. We note that the asymmetric stretch of methyl (–CH_3) groups overlaps with the methylene scissoring mode and could also contribute to the 6.9 μm feature (Silverstein & Bassler 1967). However, it is unlikely that methyl groups provide a dominant contribution to the 6.9 μm band because the 3.4 μm data (Figure 4(a)) show that methylene groups are far more abundant than methyl groups.

The position of the 6.9 μm band may provide further evidence that the observations are consistent with the presence of H_n-PAHs (Sandford et al. 2013). To determine how various baseline subtraction techniques affected the centroid determination of the 6.9 μm feature in IRAS 22272+5435, the continuum was subtracted using three different approaches before fitting with a Gaussian. The measured variations in the centroid using the different baselines was 0.0022 μm, which was about half the fitting error of the Gaussian and thus has little contribution to the centroid error. We note that because of the noisiness of the data, we are unable to reliably perform a similar fitting for IRAS 04296+3429 and IRAS 05341+0852. Ultimately, the center of the peak for IRAS 22272+5435 was determined to be at 6.901 ± 0.005 μm (1449 ± 1 cm^{-1}) (Figure 5). A similar fitting was performed on the previously collected *ISO* SWS data with an obtained centroid of 6.890 μm.

The canonical positions of the IR absorption for the methylene scissoring mode are approximately 6.811 μm (1468 cm^{-1}) for linear aliphatic compounds and 6.887 (1452 cm^{-1}) for cyclic aliphatic molecules (e.g., cyclohexane). The redshifting of the methylene scissoring mode between linear and cyclic aliphatics is due to an increased level of molecular strain. As previously stated, adjacent aliphatic and aromatic moieties result in increased strain, which further

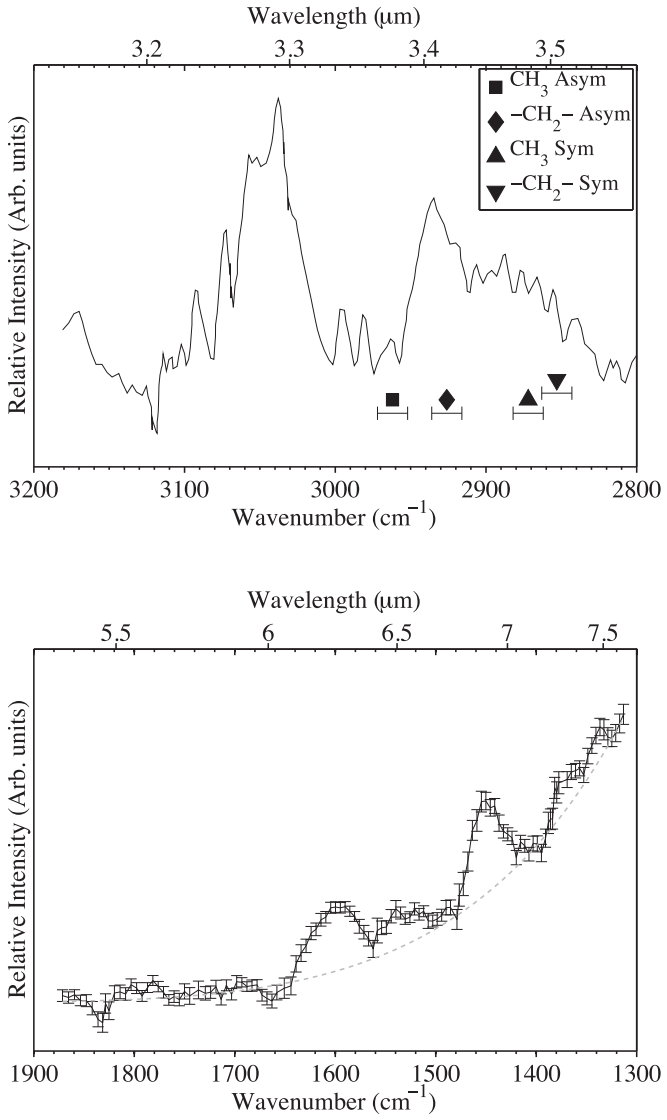

Figure 4. Infrared emission spectra of IRAS 22272+5435. (Top) 3.3 and 3.4 features from Geballe et al. (1992). (Bottom) 5.34–7.61 μm SOFIA spectral observations. The dashed line represents an estimated baseline used for the corrected spectrum and fitting of the 6.9 μm feature in Figure 5. The data used to create this figure are available.

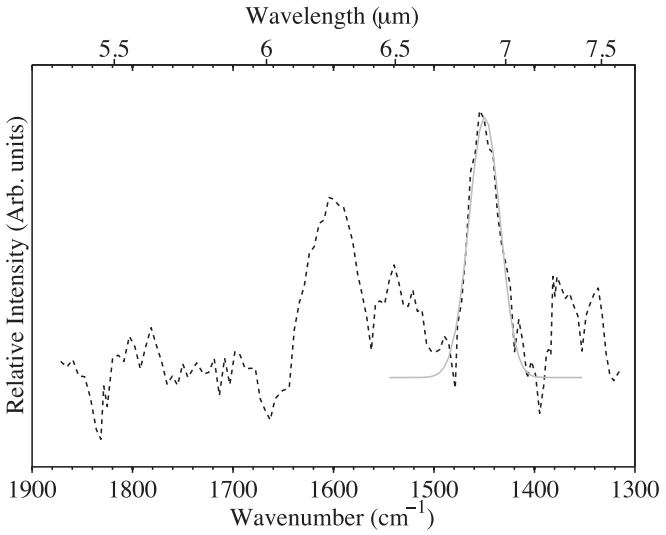

Figure 5. Baseline corrected infrared spectra of IRAS 22272+5435 with a Gaussian ($y = 5.837e^{-\frac{(x-6.899)^2}{2(0.0736)^2}}$) fitted to the 6.9 μm feature. The data used to create this figure are available.

redshifts this band position (Silverstein & Bassler 1967). The 6.9 μm emission feature in IRAS 22272+5435 was found to have a precise position of 6.890–6.901 μm (1449 cm^{-1}). The redshifting of this band from the canonical positions of the methylene scissoring mode in absorption may be consistent with the presence of H_n-PAH molecules with a fairly low level of strain, but may also be a consequence of anharmonicity from excited state emission. Anharmonicity is known to redshift the positions of PAH emission features by $\sim$15 cm^{-1} relative to absorption (Bauschlicher et al. 2008), and work by Baughcum & Leone (1980) suggests that it will also cause a slight redshift in the position of the methylene scissoring mode. The current data do not allow us to make a determination of whether the hydrogenation is lightly spread across many PAH molecules, or it is constrained to a smaller population of more heavily hydrogenated molecules. Since the precise position of the 6.9 μm band for IRAS 22272+5435 suggests little to no additional strain beyond what is found in simple cyclic aliphatic molecules, we hypothesize that the aliphatic moieties may be located contiguously within the H_n-PAHs because contiguous aliphatic groups would minimize the strain caused at the interface of aromatic and aliphatic moieties.

4. Conclusion

Mid-infrared observations (5.34–7.61 μm) of three protoplanetary nebulae with abnormally large 3.4 μm emission features and one protoplanetary nebula with typical emission features were collected using the FORCAST instrument on SOFIA during the same observation flight. All of the objects with abnormally large 3.4 μm bands were shown to also possess an emission feature at 6.9 μm, while the typical emitter did not. The band positions of the 3.4 μm features suggest that the objects contain hydrocarbons with an abundance of strained methylene and far fewer methyl moieties. The presence of a 6.9 μm feature and the exact position of the band in IRAS 22272+5435 observed in these SOFIA data further supported this assessment.

H_n-PAHs are hypothesized to be the source of these emission features. These compounds make an excellent candidate because they are cyclic in nature and possess few methyl groups. Additionally, the combination of neighboring aromatic and aliphatic moieties creates ring strain, which could explain the slightly blueshifted C–H stretch bands at 3.4 μm and the slightly redshifted methylene scissoring bands at 6.9 μm. Future observations that provide improved signal-to-noise are required to confirm the exact band positions for objects significantly fainter than IRAS 22272+5435. Because the position of this band in emission may also be influenced by anharmonicity, more studies that characterize the magnitude of this effect are crucial.

Because the 6.9 μm band position is sensitive to ring strain, more precise band positions from these observations that accurately account for anharmonicity could help to determine whether the aliphatic features are due to excess hydrogen sparsely spread across larger numbers of mostly aromatic molecules or whether they are constrained to a relatively

smaller population of more heavily hydrogenated molecules. We hypothesize that in the former case, there is comparatively more strain when aliphatic groups are sparse and frequently intermixed with aromatic groups, leading to a greater redshift of the 6.9 μm band. Furthermore, we hypothesize that in the latter case, heavy hydrogenation may result in molecules with multiple aliphatic groups that are adjacent to one another leading to locally reduced strain and a 6.9 μm band that is more consistent with ordinary cyclic aliphatics.

Importantly, the upcoming arrival of the *James Webb Space Telescope* (*JWST*) may be an important step for continued progress on this research. The increased sensitivity of *JWST* should enable collection of spectra from post-AGB objects with improved signal-to-noise. More importantly, *JWST* should allow for the simultaneous collection of 3.4 and 6.9 μm features in suitable post-AGB objects. This will enable deeper analysis, including direct comparison of band intensities from features near 3 μm and those at longer wavelengths including the 6.9 μm band to demonstrate correlations. Collectively, these data should help clarify the validity of the H_n-PAH hypothesis.

This material is based upon work supported by the National Aeronautics and Space Administration through the NASA Astrobiology Institute under Cooperative Agreement Notice NNH13ZDA017C issued through the Science Mission Directorate. We would also like to thank the reviewers of this manuscript for their thoughtful comments. Additionally, this work was based in part on observations made with the NASA/DLR Stratospheric Observatory for Infrared Astronomy (SOFIA). SOFIA is jointly operated by the Universities Space Research Association, Inc. (USRA), under NASA contract NAS2-97001, and the Deutsches SOFIA Institut (DSI) under DLR contract 50 OK 0901 to the University of Stuttgart.

ORCID iDs

Christopher K. Materese https://orcid.org/0000-0003-2146-4288

References

Adams, J. D., Herter, T. L., Gull, G. E., et al. 2010, Proc. SPIE, 7735, 77351
Allamandola, L. J., Bregman, J. D., Sandford, S. A., et al. 1989a, ApJ, 345, L59
Allamandola, L. J., Hudgins, D. M., & Sandford, S. A. 1999, ApJL, 511, L115
Allamandola, L. J., Tielens, A. G. G. M., & Barker, J. R. 1989b, ApJS, 71, 733
Baughcum, S. L., & Leone, S. R. 1980, JChPh, 72, 6531
Bauschlicher, C. W., Peeters, E., & Allamandola, L. J. 2008, ApJ, 678, 316
Geballe, T. R., Tielens, A. G. G. M., Kwok, S., et al. 1992, ApJ, 387, L89
Goto, M., Kwok, S., Takami, H., et al. 2007, ApJ, 662, 389
Herter, T. L., Adams, J. D., De Buizer, J. M., et al. 2012, ApJL, 749, L18
Hrivnak, B. J., Geballe, T. R., & Kwok, S. 2007, ApJ, 662, 1059
Peeters, E., Hony, S., van Kerckhoven, C., et al. 2002, A&A, 390, 1089
Sandford, S. A., Bernstein, M. P., & Materese, C. K. 2013, ApJS, 205, 8
Silverstein, R. M., & Bassler, G. C. 1967, Spectrometric Identification of Organic Compounds (2nd ed.; New York: Wiley)
Tielens, A. G. G. M. 2008, ARA&A, 46, 289
Wexler, A. S. 1967, ApSRv, 1, 29
Young, E. T., Becklin, E. E., Marcum, P. M., et al. 2012, ApJL, 749, L17